

Article pubs.acs.org/EF

Elucidation of Low Molecular Weight Polymers in Vehicular Engine **Deposits by Multidimensional Mass Spectrometry**

Savannah R. Snyder and Chrys Wesdemiotis*



Cite This: Energy Fuels 2021, 35, 1691-1700



ACCESS I

III Metrics & More



Article Recommendations



Supporting Information

ABSTRACT: Engine oil is mainly comprised of base oils and various additives, which are low molecular weight polymers mixed into the oil resulting in a polymer blend. Dispersants and detergents, the two most abundant additives, are intended to keep the engine free of particulate but are not always successful. At high temperatures, species not combusted may undergo oxidation and degradation or create other byproducts, generating particulate deposition. Knowledge of the molecular makeup of these byproducts is essential, as particulate accumulation can cause serious issues to the engine and ultimately to the operator. In this study, unknown deposits from the air-intake valve of a vehicular engine have been analyzed via a palette of mass spectrometry (MS) methods, including matrix-assisted laser desorption/ionization MS with postacquisition data processing, atmospheric solids analysis probe MS, and electrospray ionization MS interfaced with 2D separation via reversed-phase liquid chromatography and ion mobility spectrometry. Low molecular weight, aminated poly(propylene glycol) and polyisobutylene detergents and a poly(methyl methacrylate) viscosity modifier were conclusively identified in the deposit, along with oxidized polyethylene chains leaked into the oil/additives blend from vehicular tubing and tanks. The use of different methods was essential for the confident elucidation of the low molecular weight macromolecules giving rise to the vehicular engine particulates.

■ INTRODUCTION

Internal combustion engines are utilized worldwide, but the understanding of the chemical processes occurring within them, from air-intake mixing with fuel, to oil lubrication and its additives, to combustion, remains marginal. The high heats and pressures necessary for combustion impart a large amount of energy that can cause ancillary reactions and problems with future combustion and air-intake. One major concern is stochastic preignition (SPI), an untimely ignition event prior to ignition of the main fuel charge, which is thought to be caused by particulate/droplets within the combustion chamber.² Several experimental studies have been performed to both understand and prevent such untimely combustion³ as well as determine the cause of engine particulate deposits,6-9 though there is still disagreement whether these particulates could remain after a few ignition cycles. 10 Overall, deposit analysis has been neglected compared to other issues, like SPI, engine knocking, or super knocking. 11,12

Engine deposits are presumably produced from interactions with engine oil, which mainly consists of hydrocarbonaceous material (paraffins, polycyclic aromatic hydrocarbons [PAHs], naphthenes, etc.); however, various additives, often referred to as a "performance package", are also present (Table 1).13 These additives are generally low molecular weight polymers

Table 1. Major Components of Motor Oil Packages¹³

motor oil component	%
base oils	75-95
viscosity index improvers	5-10
additive package	8-15

that encompass dispersants, detergents, antioxidants, antiwear agents, viscosity modifiers, and friction modifiers, which impart advantageous properties to the oil, usually based on their structural responses to stimuli like temperature. Poly(ether amines) (PEAs) and poly(isobutylene amines) (PIB-amines) are typical detergents, added to prevent deposition, 14 while poly(dimethylsiloxane) and poly(methyl methacrylate) act as antifoaming agents, dispersants, or viscosity modifiers. 15 These low molecular weight polymer additives (Table 2) keep engines running efficiently with less complications. 13,16 Nevertheless, as noted previously, the additives do not always perform as expected, resulting in engine deposits liable to cause future problems. For this reason, structural characterization of these unknown deposits is imperative in the automotive industry.

While fuel and lubricant components are largely nonpolar (cf. Table 1), the more polar ingredients are often responsible for the formation of engine deposits 17 due to their heteroatom functionality (primarily amines, thiols, and ethers), which promotes attractive intermolecular interactions and aggregation. These deposits compromise engine performance, making necessary their identification, so that cleaner burning fuels can be developed. Mass spectrometry (MS) provides compositional and structural information by generating and analyzing

Received: August 11, 2020 December 11, 2020 Revised: Published: December 29, 2020





Table 2. Polymer Additives in Engine Oil and Their Applications¹¹

polymer structure	polymer name	application
$-[Si(CH_3)_2-O]_n-$	poly(dimethylsiloxane)	antifoaming agent, dispersant
$-[O-CH_2-CH(CH_3)]_n-$	poly(propylene glycol)	detergent
$-\left[\mathrm{CH_2} - \mathrm{C}(\mathrm{CH_3})_2\right]_n -$	poly(isobutylene)	detergent, dispersant
-[CH2-C(CH3)(COOCH3)]n-	poly(methyl methacrylate)	viscosity modifier

ions, a process that is generally more easily applied to polar, heteroatom containing molecules; hence the more polar engine deposits are uniquely amenable to this technique.

Various mass spectrometry methods have been used for the analysis of petroleum-based fuels and lubricants, ^{17,18} including tandem mass spectrometry (MS/MS), liquid chromatography-MS (LC-MS), ion mobility-MS (IM-MS), and atmospheric solids analysis probe-MS (ASAP-MS). ^{19–22} The most recently introduced ASAP-MS technique²³ allows for the direct analysis of liquid and solid samples with little to no sample preparation.²⁴ This feature makes ASAP-MS particularly appealing for the analysis of fuels and fuel byproducts, as it bypasses solubility issues and time-consuming extraction processes. ^{25,26} MS/MS, LC-MS, and IM-MS can also provide useful analytical information about these samples; specifically, MS/MS can reveal connectivity insight about the ions observed by MS,27 whereas the LC and IM event add necessary separation dimensions to deconvolute complex spectra. 18,27,28 Several of these techniques can also be interfaced with one another to reduce sample complexity, speed up the analysis, and augment the derived structural information. For example, ASAP-IM-MS has been employed for the rapid analysis of lubricants, 25 while LC-MS/MS has aided the identification of the functional groups in fuels.² Collaborative application of multiple techniques, in series (i.e., hyphenated on the same instrumentation) or in parallel (i.e., using different instruments) not only provides an added dimension of separation, but also unveils multiple chemical properties, including primary structure (via MS/MS), polarity (via LC), and 3D shape (via IM), which facilitates the analysis of inherently complex samples, like fuels and lubricants/ additives. In this study, such a multidimensional approach was utilized to characterize deposition solids in vehicular engines using petroleum by matrix-assisted laser/desorption ionization mass spectrometry (MALDI-MS), ASAP-MS, LC-IM-MS, and a postacquisition data evaluation method (Kendrick Analysis).²⁹ These techniques were used collaboratively in order to gain a comprehensive understanding of the unknown deposit for future prevention.

MATERIALS AND METHODS

The solvents used for mass spectrometry analysis, methanol (MeOH) and tetrahydrofuran (THF), were acquired from Fisher Chemical (Fair Lawn, NJ). Sodium trifluoroacetate (NaTFA; Fluka Analytical, St. Louis, MO) and trans-2-[3-(4-tert-butylphenyl)-2-methyl-2-propenylidene]malononitrile (DCTB; Sigma-Aldrich, St. Louis, MO) served as cationizing salt and matrix, respectively, in the MALDI-MS experiments. All chemicals were used as received. The samples analyzed were obtained from an industrial automotive company (proprietary) as black solids; they were collected from the head of the air-intake valve of engines run on fossil fuel after traveling distances of >100 km. Due to the unknown composition of the solids, and comparative engine oil guidelines, the samples were handled with extreme care, using adequate personal protective equipment (PPE).

MALDI-MS Experiments. MALDI mass spectra were recorded on a Bruker UltraFlex III MALDI tandem time-of-flight (ToF/ToF) mass spectrometer (Bruker, Billerica, MA) equipped with a Nd:YAG

laser emitting at 355 nm. The instrument was operated in positive ion reflectron mode (resolving power ~25 000 fwhm). Black, solid samples retrieved from engine in-take valves were extracted into THF for MALDI-MS analysis; 10 mg was mixed with 1 mL of THF to form analyte solutions at an approximate concentration of 10 mg mL $^{-1}$ (partial solubility). DCTB was dissolved in THF at 20 mg mL $^{-1}$, and NaTFA in MeOH at 10 mg mL $^{-1}$; these solutions were mixed in the ratio 10:1 (v/v), and ~1 μ L of the resulting mixture was spotted onto the MALDI target plate and allowed to dry under ambient conditions. Subsequently, ~1 μ L of analyte solution was deposited on top of the dry matrix/salt spot, followed by another deposition of ~1 μ L of matrix/salt solution on top of the dry sample (sandwich method). Sodiated poly(methyl methacrylate) ($M_{\rm n}=2000$ Da) was used for same day calibration. Bruker's FlexAnalysis software was used for data analysis.

Post-Acquisition Data Analysis. Kendrick analysis of the MALDI-MS data was performed by importing the raw data retrieved from the FlexAnalysis software into an Excel program developed at AIST (Advanced Industrial Science and Technology, Tsukuba, Japan). The Kendrick mass (KM) values of the observed ions were calculated according to eq 1, in which R/x is the fractional base unit ($x \ge 1$) used to create Kendrick plots and m/z the ion's mass-to-charge ratio. The corresponding Kendrick mass defects (KMDs) were obtained according to eq 2, i.e., by subtracting the KM from the nominal mass of the ion (NKM). Kendrick displays were derived by plotting Kendrick mass defect (KMD) vs m/z. The best visualization (i.e., optimal separation of the detected polymer distributions) was achieved using R = 100.052 (IUPAC or exact mass of a PMMA repeat unit) and x = 1.

$$KM = \left(\frac{m}{z}\right) \left(\frac{\text{round}\left(\frac{R}{x}\right)}{\frac{R}{x}}\right) \tag{1}$$

$$KMD = NKM - KM \tag{2}$$

LC-IM-MS Experiments. LC fractionation of the engine deposit was performed using an ACQUITY ultraperformance liquid chromatography (UPLC) ethylene bridged hybrid (BEH) C18 column (50 \times 2.1 mm; 1.7 μ m particles) on a Waters ACQUITY UPLC system hyphenated to a Waters Synapt HDMS quadrupole/ time-of-flight (Q/ToF) mass spectrometer (Waters, Milford, MA). Aliquots from the partially soluble 10 mg mL⁻¹ THF extract were diluted with methanol prior to LC-MS to obtain solutions with an approximate concentration of 0.01 mg mL⁻¹ in 9:1 MeOH:THF (v/ v). NaTFA was added as a cationizing agent to aid in the ionization of the polymeric species present. The samples were filtered with an Acrodisc syringe filter (polyvinylidene difluoride membrane, diameter 13 mm, pore size 0.2 μ m) before analysis. A gradient elution protocol was applied, using mobile phases A (water with 0.1%, v/v, formic acid) and B (methanol with 0.1%, v/v formic acid). 18 Solvent composition was changed as follows: 80% B for 0-0.5 min, 100% B for 0.5-10.0 min, and column flushing with 100% B for 10.0-15.0 min. 18 The injection volume, column oven temperature, and flow rate were 10 μ L, 50 °C, and 0.5 mL min $^{-1}$, respectively. The eluates were directly fed into the electrospray ionization (ESI) source of the mass spectrometer, which was operated under the following conditions: positive ion mode (resolving power ~30 000 fwhm); ESI potential, 3.8 kV; sample cone voltage, 60 V; extraction cone voltage, 3.8 V; source temperature, 80 $^{\circ}\text{C};$ desolvation gas (N_2) temperature, 150 $^{\circ}$ C; desolvation gas flow rate, 700 L h $^{-1}$.

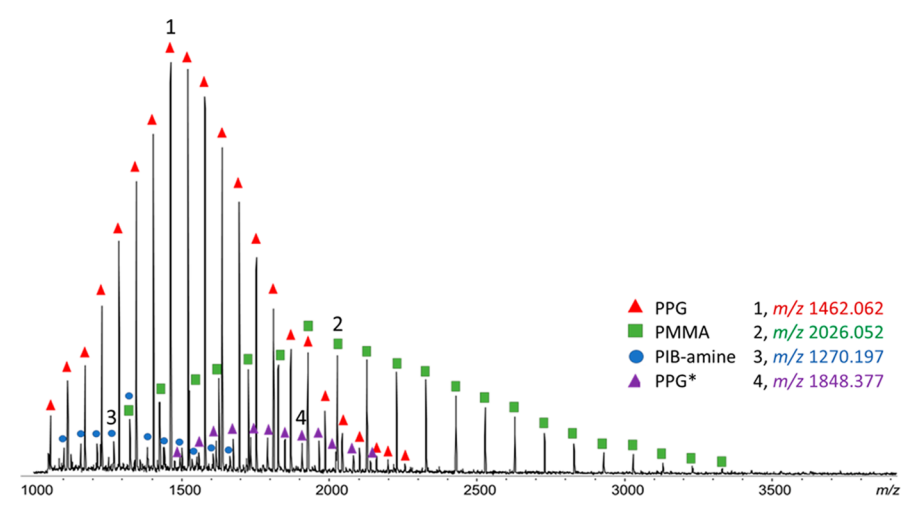


Figure 1. MALDI-MS spectrum of an unknown engine deposit obtained from the air-intake valve of a vehicular engine. The polymer distributions observed are labeled by different signs; the numbers 1–4 indicate single oligomers from each distribution, which are discussed in the text.

The Synapt Q/ToF mass spectrometer is equipped with a traveling wave (TW) ion mobility (IM) functionality between the Q and ToF mass analyzers. 32 LC-IM-MS experiments were run by applying a TW field to the IM cell which was pressurized with N_2 bath gas at a flow rate of 22.7 mL min $^{-1}$; the TW height and TW velocity were 7 V and 350 m s $^{-1}$, respectively.

ASAP-MS Experiments. ASAP-MS experiments were run on the Synapt Q/ToF mass spectrometer (vide supra) by switching the ESI with the Waters ASAP source; the latter source provides a hot stream of nitrogen gas (flow rate 900 L h⁻¹), whose temperature can be adiusted between 50 and 500 °C to cause desorption and thermal degradation of the sample, which is mounted on a glass capillary. The ASAP source is equipped with an atmospheric pressure chemical ionization (APCI) device (corona discharge) for in situ ionization of the desorbates and degradants. A black, solid sample was applied to the ASAP capillary by dipping it into the engine deposit. Methanol was placed in the source in a 20 mL vial to induce protonation. The temperature of the N₂ stream was increased gradually within 50-500 °C over 15 min, at a rate of 50 °C min⁻¹ from 50 to 200 °C (first 3 min) and 25 °C min⁻¹ from 200 to 500 °C (minutes 3-15). Subsequently, isothermic runs were continued at 500 °C until ionization was no longer observed.

■ RESULTS AND DISCUSSION

MALDI-MS Fingerprinting of Engine Deposit Extract.

The engine deposit investigated gave rise to four polymer distributions upon MALDI-MS analysis (Figure 1). The major distribution is annotated with red triangles and has a 58-Da repeating unit. This repeating unit mass corresponds to a poly(propylene glycol) (PPG), a widely used detergent in fuels/lubricants, especially when harboring amine functionalities at its chain ends; such PPGs are referred to as polyether amines. ¹⁴ As an oxygen rich polymer, PPG is readily ionized by Na⁺ adduction. ^{33–35} For this reason, a sodium salt was used as cationization agent in the MALDI-MS experiments (vide supra). Accurate mass measurement of the [M + Na]+ ions in the major PPG distribution confirms a summed end group mass of 58n + 46 Da, which agrees well with the polyether diamine connectivity $H_2NCH_2CH_2-[OCH_2CH(CH_3)]_n$ $OCH_2CH_2NH_2$ (summed end groups mass of 58 + 46 = 104 Da; C₄H₁₂N₂O). For example, the calculated monoisotopic m/z ratio for the 23-mer of this PPG is 1462.048, which matches within <10 ppm the measured value of 1462.062. It should be noted at this point that accurate mass measurement corroborates the diamine nature of the main

distribution but not necessarily the above given sequence; the two ethylene oxide units required to account for the measured mass were arbitrarily placed at the chain ends but could also be located in central positions. Sequence analysis might be possible via MS/MS,³⁵ but this elaborate issue is beyond the scope of this study.

A further, minor PPG distribution of [M + Na]⁺ ions appears 38 Da higher in mass than adjacently located oligomers of the major product described above. It has been labeled with purple triangles in Figure 1 and is denoted as PPG* for differentiation. Accurate mass measurement reveals a summed end group composition of C_6H_{12} , 84 Da (= 58 + 26 Da), strongly suggesting the chain connectivity C₆H₁₁- $[OCH_2CH(CH_3)]_n$ -H. The sodiated 30-mer of this distribution is observed at m/z 1848.377, which agrees well with the calculated monoisotopic m/z of 1848.340. It is worth mentioning again, that our mass analysis only indicates the total end group mass and a plausible composition, not how the elements of C₆H₁₂ may be split among the two end groups; in the chain structure shown, the entire C_6 moiety was attached at one chain end to maintain a PPG repeating unit at the other chain end.

The second most intense distribution (green squares) has a 100-Da repeat unit, indicative of poly(methyl methacrylate) (PMMA), a known viscosity modifier. PMMA is also sodiated upon MALDI due to its oxygen rich backbone. The accurate m/z values of the $[M + Na]^+$ ions from this product indicate a summed end group mass of 100n + 2 Da, consistent with the chain structure $H-[CH_2C(CH_3)(COOCH_3)]_n-H$. The calculated monoisotopic mass of the sodiated 20-mer is 2026.054, which is in excellent agreement with the measured m/z of 2026.052 (1 ppm difference). This PMMA distribution shares an isobaric oligomer with the major PPG distribution at m/z 1926, where the $[M + Na]^+$ ions from PMMA₁₉ (monoisotopic mass of 1926.002) and diamine-capped PPG₃₁ (1926.382) overlap. This adds complexity to the spectrum, necessitating further separation (vide infra).

The least abundant of the detected distributions has a repeat unit of 56 Da, indicative of polyisobutylene (PIB), a known oil detergent. Generally, PIB is capped with amine group(s) when applied in fuel additives (vide supra). This, and any other heteroatom functionalities added, make PIB ionizable by MALDI. As a nonpolar, saturated polymer, PIB would be

otherwise difficult to observe by MALDI-MS, which explains the low intensity of its distribution. Amine functionalization can make low mass oligomers observable as $[M + H]^+$ ions.³⁶ The MALDI-MS data (Figure 1, blue circles) indicate a summed end group mass of 56n + 36 Da. A recently invented family of PIB amines reconciles this result;³⁷ they carry amine and ether substituents that would enable ionization by protonation and, hence, MS detection in the form of M + H]+ ions. Our MALDI-MS analysis is consistent with a PIB amine having the structure 37 CH₃-[CH₂C(CH₃)₂]_n-CH₂CH-(OH)CH(CH₃)CH₂-[N(CH₃)CH₂]₃-NHCH₃ (total end group mass = $56 \times 4 + 36 = 260$ Da). The 18-mer of this polymer has a calculated monoisotopic m/z of 1270.392, which agrees within 0.016% with the measured m/z of 1270.197; the mass accuracy for this low-intensity, near noise level distribution is expectedly poorer than for the other polymers observed in the deposit. This problem is convoluted by isobaric overlap of $[M + H]^+$ from PIB_{19} amine (m/z)1326.455) and $[M + Na]^+$ from PMMA₁₃ (m/z 1325.687). Because of such isobar superposition, which is observed multiple times in the m/z 1000–2000 range, the MALDI-MS spectrum was processed by Kendrick analysis to better visualize the composition of the polymer blend in the engine deposit studied.

Modified Kendrick Analysis. Kendrick analysis usually calculates mass defects by normalizing masses relative to the mass of CH₂, which serves as base unit (14.01565 is set equal to 14.00000). The modified approach employed here normalized masses (or m/z ratios) using a fraction of a polymer repeat unit (R/x), cf. eq 1. Using such fractional base units has been shown to intensify separation among the components of a (co)polymer blend, thereby providing a better picture of sample composition and of minor variations among different samples.^{38,39} It should be noted that Kendrick analysis is generally performed with m/z data measured with very high mass accuracy, as available with spiral-ToF or Fourier transform MS instrumentation; nevertheless, m/z data obtained with the ToF/ToF mass spectrometer utilized here also provide adequate Kendrick plots that reveal valuable compositional insight, as demonstrated in Figure 2, which was obtained with R = 100.05243 (monoisotopic IUPAC mass of

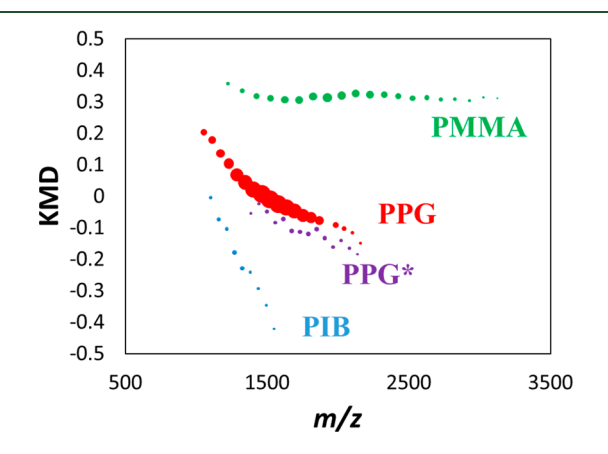


Figure 2. Kendrick plot of the unknown engine deposit contents as observed by MALDI-MS and visualized by Kendrick analysis (using *R* = 100.05243 as base unit). Each sign represents a single oligomer and sign size is proportional to the oligomer's relative abundance in the MALDI-MS spectrum. The four polymer distributions observed (PMMA, PPG, PPG*, and PIB) are labeled in different colors.

the PMMA repeat unit) and x = 1. Application of this R/x base unit enabled clear, visual separation of three different homopolymers coexisting over a 1000 Da range in the polymer blend analyzed (PPG, PMMA, and PIB). Subtle separation of two homopolymers differing only in their end groups (i.e., PPG and PPG*) was also achieved. A comparable visual representation was obtained with R = 58.04186 (monoisotopic IUPAC mass of the PPG repeat unit) and x = 1, cf. Figure S1. Both plots show approximately horizontal alignment for the polymer selected for the R/x base unit, validating the identity of this polymer.³¹

ASAP-MS of Engine Deposits. Insolubility can be a discriminating factor when analyzing deposited particulate. To circumvent the issue, ASAP-MS was employed, which can ionize solid samples via thermal desorption and/or thermal degradation depending on sample volatility and ASAP temperature. ASAP-MS has been performed by other groups to examine crude oil and gasoline additives, 25,26,40,41 focusing on the molecular weight distribution (MWD) of the products 40,41 and characterization of the ion distributions resulting from known, authentic polymeric additives in petroleum. 25,26 Here, the ASAP-MS method is applied for the first time to unknown solid vehicular engine deposits to characterize the types of polymers present in such samples and also assess their molecular structure identities. ASAP-MS experiments were run using thermometric gradient ramping or isothermic conditions. Temperature is the most vital parameter in ASAP-MS, comparable to the mobile phase in liquid chromatography. Separation is dictated by the differing boiling points of the materials present. During a 50-500 °C ramp over 15 min, volatilization of the sample began at approximately 325 °C (cf. Figure 3a). The mass spectrum extracted at this temperature shows two PPG distributions of similar intensity (Figure 3b). One consists of low mass PPG oligomers with the same end group substituents as the main PPG distribution observed in the MALDI-MS spectrum (cf. peaks labeled by red triangles in Figures 1 and 3b). Under ASAP conditions, this polyether diamine forms [M + H]+ ions, with the 7-mer appearing at m/z 511.400 which matches within 8 ppm the theoretically expected value of 511.396 for this chain size. The second PPG distribution is labeled by green upside-down triangles and corresponds to PPG with H- and -OH end groups. The $[M + H]^+$ ion of its 9-mer is observed at m/z541.397, which agrees very well with the calculated m/z of 511.395 (4 ppm difference). These low mass PPGs were not detected in the MALDI-MS experiment due to matrix interferences in the same mass region.

Very similar ASAP-MS spectra were extracted above 325 $^{\circ}$ C; however, at the higher temperatures, thermal degradation becomes progressively prominent, leading to increased intensities of low mass ions that differ by a CH₂ (14 Da) unit (vide infra). In fact, the rise in total ion intensity at \sim 14 min (Figure 3a) mainly results from such degradants.

In order to observe higher boiling point material without the noise of low mass 14-Da distributions, an isothermic 500 °C "bake-out" was carried out for the engine deposit (cf. Figure 4a). The sample was introduced to the ASAP source at 500 °C (maximum possible) and allowed to volatilize/desorb until ions were no longer observed. The first peak at 0.75 min confirmed the presence of the polymers described above (Figure 3b). Conversely, the mass spectrum extracted from the peak at 1.35 min reveals a PIB distribution, cf. Figure 4b, on top of degradant noise with a 14-Da repeat unit. The exact m/z

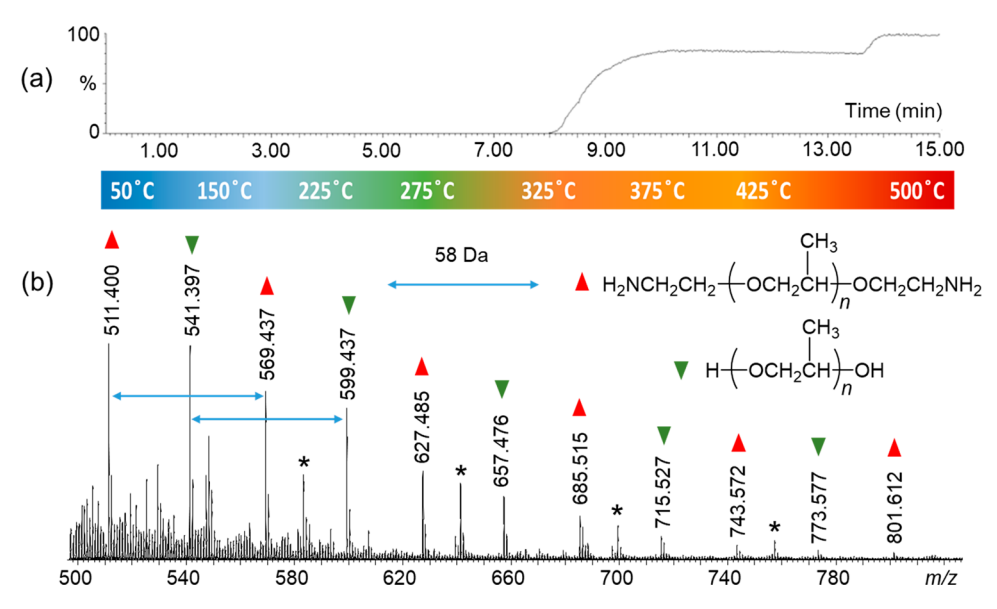


Figure 3. (a) ASAP-MS thermogram of the unknown engine deposit from 50 to 500 °C, indicating that volatilization and thermal desorption starts at \sim 325 °C. (b) Extracted mass spectrum from 8.00 to 8.50 min (m/z 500–1000 range), showing two PPG distributions (58-Da repeat unit) and their structures. A minor third distribution (marked by *) arises from a PIB (56-Da repeat unit) discussed with Figure 4.

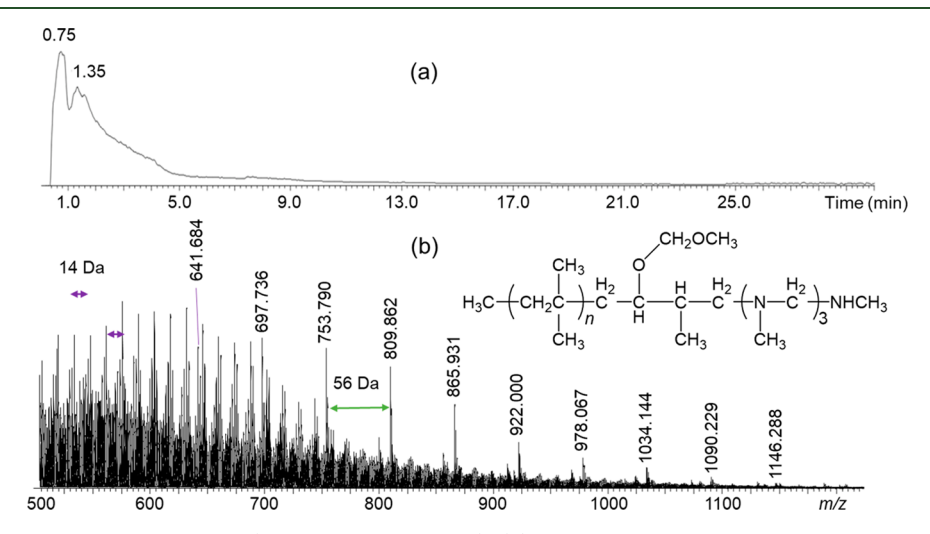


Figure 4. (a) Isothermic ASAP-MS thermogram (500 °C held for 30 min). (b) Mass spectrum extracted from the peak at 1.35 min, where a PIB distribution is detected.

values of the PIB product indicate a similar composition to that observed upon MALDI-MS plus one C_2H_4O unit; a plausible structure is included in Figure 4b. The protonated 8-mer of this PIB has a theoretical monoisotopic m/z ratio of 753.792 and is detected at m/z 753.790 (3 ppm agreement), providing credence for the proposed structure. The extra C_2H_4O unit was attached as a $-CH_2OCH_3$ ether to the OH group of the PIB found by MALDI-MS, viz. $CH_3-PIB-CH_2CH(OH)CH-(CH_3)CH_2-[N(CH_3)CH_2]_3-NHCH_3$, but might alternatively be present as a $-CH_2CH_2O-$ segment within the main chain of the polymer. It is unlikely that the C_2H_4O unit is attached as a $-CH_2CH_2OH$ end group, as such a moiety would easily lose water at the temperature used.

The products released from the engine deposit by isothermic heating at 500 $^{\circ}$ C for longer times were also examined. The mass spectra extracted from the ASAP-MS thermogram in Figure 4a at 2–6, 6–10, and 10–14 min are depicted in Figures S1a,b and S2, respectively. In the 2–6 and 6–10 min windows, PPG diamine (labeled by red triangles in Figure S2)

as well as a thermal decomposition product of this compound (blue squares) are observed. Expectedly, the PPG diamine oligomers volatilized at 500 °C have longer chains than those volatilized at 325 °C, cf. Figure S2 vs 3b. The thermal degradant is missing the elements of NH₃, indicating that ammonia elimination from one chain end proceeds efficiently during prolonged heating at 500 °C. It is noteworthy that the PPG diamine is only observed in protonated form, viz. $[M + H]^+$, whereas the degradant gives rise to a mixture of protonated ions $([M + H]^+)$, radical cations $(M^{+\bullet})$, and immonium cations $([M - H]^+)$; all three of the latter species can be formed during atmospheric pressure chemical ionization (APCI) of amines. ⁴²

Increasing the exposure time at $500\,^{\circ}$ C from 2-6 to 6-10 min changes the resulting ASAP-MS spectrum only slightly (cf. Figure S2b vs S2a). The PPG diamine distribution appears to gain in relative intensity as time increased at constant temperature. This trend suggests that this distribution has a slightly higher boiling point than the degradation product,

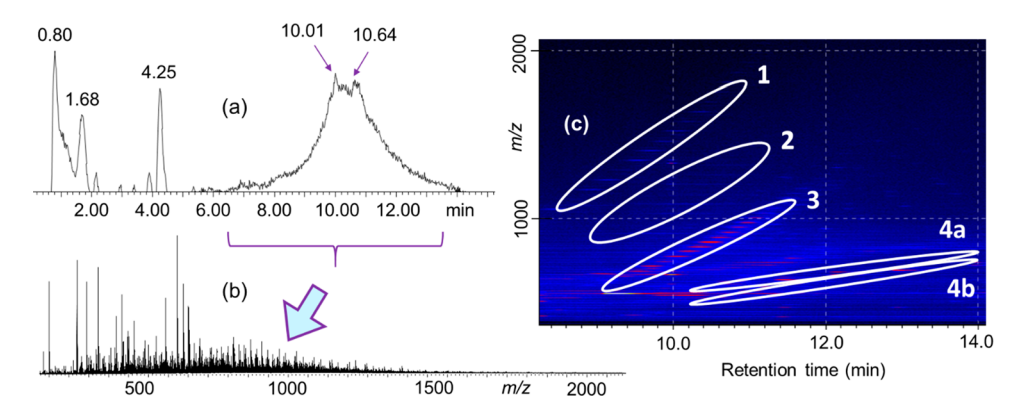


Figure 5. (a) LC-MS total ion chromatogram of the unknown engine deposit. (b) LC-MS spectrum extracted from the broad peak stretching from 6 to 14 min; see Figures S4 and S5 for the mass spectra extracted from the peaks at 1.68 and 4.25 min, respectively. (c) 2D LC-IM mobilogram of the engine deposit, showing five polymer distributions, which have been encased in ovals (see Figure S6 for a mobilogram in warmer colors); the mass spectra extracted from the encased LC-IM bands are shown in Figures 6 and 7.

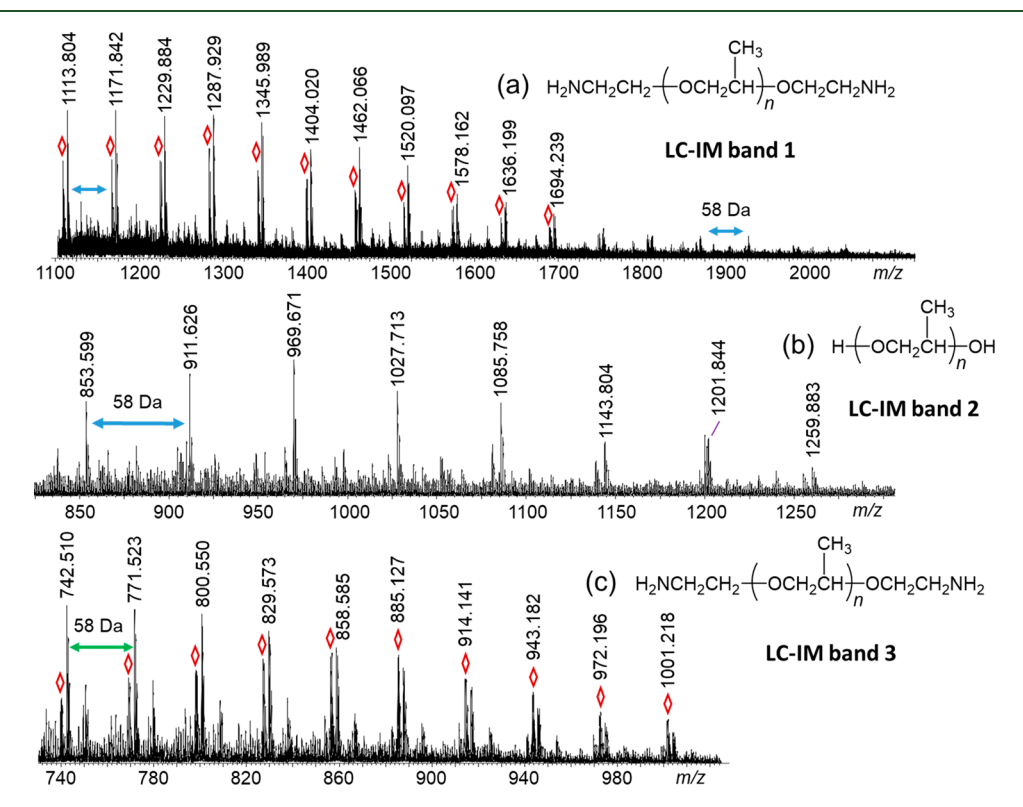


Figure 6. LC-IM-MS spectra extracted from bands 1–3 of the mobilogram in Figure 5c, showing (a,b) singly or (c) doubly charged PPG distributions with (a,c) diamine or (b) H/OH end groups. (a) $[M + Na]^+$ ions at the marled m/z values and $[M + NH_4]^+$ ions (labeled by \diamondsuit) 5 m/z units lower. (b) $[M + Na]^+$ ions and their m/z values. (c) $[M + 2Na]^{2+}$ or $[M + Na + NH_4]^{2+}$ ions and their m/z values; the ammoniated species are labeled by \diamondsuit . The mass difference between adjacent oligomers is 58 Da (mass of PPG repeat unit) in all spectra; the m/z distance between adjacent oligomers is (a,b) 58 and (c) 29 m/z units.

consistent with its more polar end groups vis à vis those of the degradant. Different end groups on the same bulk polymer evidently have an effect on the physical properties, if the overall molecular weight is low.

At even longer heating times solely degradation products are observed, as attested by the spectrum in Figure S3, which was acquired from the oligomers released from the engine deposit during 10–14 min heating at 500 °C. Now, only the degradation product of PPG diamine is observed (blue squares in Figure S3), along with an additional PPG degradant (orange triangles), having C_3H_5- and -H end groups; the latter degradant may originate from the PPG* component detected

upon MALDI-MS (vide supra). Surprisingly, the 10–14 min heating also produced a polyethylene (PE) distribution, which is marked by red ovals in Figure S3. PE is not usually part of an additive package, but it is often used in the tubing and tanks of vehicles, ⁴³ from where it can potentially be extracted into the engine oil or fuel. This saturated hydrocarbon polymer is not detectable by MS techniques, unless it is derivatized with polar substituents. Such functionalization can, however, take place through thermal-oxidative degradation via radical intermediates in the vehicular engine ^{44,45} and/or the ASAP source. ⁴⁶ The PE oligomers detected are attributed to short, oxidized

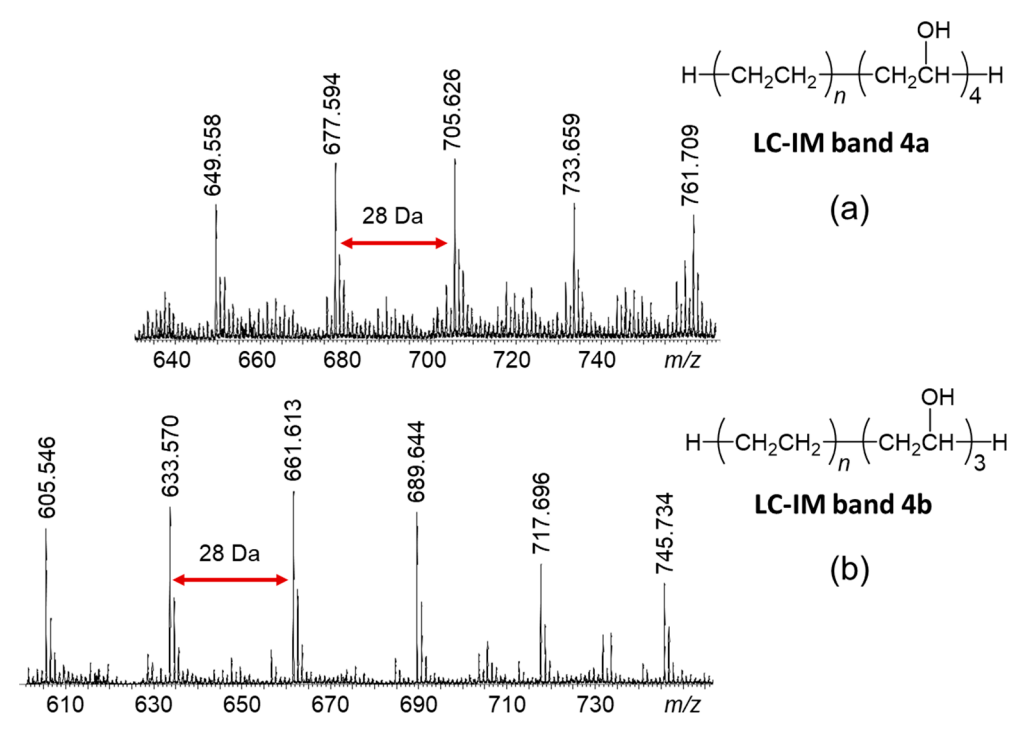


Figure 7. LC-IM-MS spectra extracted from bands 4a/4b of the mobilogram in Figure 5c, showing sodiated PE chains carrying (a) 4 or (b) 3 oxidized repeat units formed by CH₂ \rightarrow CH(OH) oxidation via radical intermediates in the vehicular engine. The ions observed at m/z (a) 761.709 and (b) 745.734 correspond to 24-mers with (a) 20 and (b) 21 unoxidized repeat units, respectively. The corresponding calculated m/z values are (a) 761.736 and (b) 745.741, respectively.

chains formed by such a process from PE leaked into the additives that ended up in the solid engine deposit analyzed.

ASAP-MS provided useful analytical information about the engine deposit, as several of the species observed by MALDI-MS could be confirmed by this orthogonal technique. The ASAP procedure is harsh, however, creating new end groups through thermal degradation. For this reason, LC-IM-MS was employed as an additional tool for the molecular structure determination of the constituents of the solid engine deposit.

LC-IM-MS Analysis of Engine Deposit Extracts. The LC-IM-MS experiments employed online multidimensional separation of the engine deposit, followed by ESI-MS characterization of the separated components. ESI permits online IM analysis of the LC eluates, which is generally impossible with MALDI. The multidimensional separation combined reversed-phase liquid chromatography (RP-LC), which fractionates based on polarity and hydrophilicity/hydrophobicity balance, 47-49 with ion mobility spectrometry, which disperses based on charge and collision cross-section (CCS is a parameter describing size and shape, analogous to hydrodynamic volume). 32,35,48-50

The RP-LC step separated the polymeric components of the engine deposit from low-molecular weight polar constituents which are eluted from the column within the first few minutes, giving rise to the fractions peaking at 1.68 and 4.25 min, cf. Figure 5a. The mass spectra extracted from these early eluting peaks confirm the presence of common engine oil additives in the engine deposit analyzed, including corrosion inhibitors, antioxidants, and friction modifiers (cf. Figures S4–S5). Increasing the mobile phase hydrophobicity caused the elution of a broad "polymer blend" peak, stretching from approximately 6 to 14 min (Figure 5a). The corresponding LC-MS spectrum (Figure 5b) shows several polymer distributions,

which cannot be confidently differentiated and interpreted due to significant overlap.

Using ion mobility as an orthogonal dimension of separation of the LC eluates enables deconvolution of the superimposed distributions, as is evident from the 2D LC-IM plot ("mobilogram") in Figure 5c. The ions present in this mobilogram can be grouped into five different bands, labeled 1–3 and 4a-4b. The corresponding LC-IM-MS spectra (Figures 6 and 7) reveal that LC-IM bands 1–3 arise from PPG oligomers with different end groups or charges, whereas bands 4a and 4b arise from PE oligomers in different levels of oxidation; a detailed spectral interpretation is provided below.

The major ion series in the LC-IM-MS spectrum of band 1 (Figure 6a) is comprised of sodiated and ammoniated (\diamondsuit) PPG oligomers with diamine end groups and a total end group mass of 104 Da (see also Figure S7). The ammoniated species appear 5 m/z units lower than the corresponding sodiated species, reflecting the mass difference between the Na⁺ and NH₄⁺ charges. The diamine-capped [PPG₁₉ + Na]⁺ ion from this distribution is observed at m/z 1229.884, which matches excellently the calculated value of 1229.880. This PPG diamine detergent has been consistently observed with all methods employed and must evidently be a major constituent of the solid engine deposit analyzed.

The PPG diamine also forms doubly charged $[M + 2Na]^{2+}$ and $[M + Na + NH_4]^{2+}$ ions, which are detected in LC-IM band 3; the LC-IM-MS spectrum extracted from this band (Figure 6c) expectedly shows n-mers every $29 \ m/z$ units (58/2) in accordance with the 2+ charge state of this distribution (see also Figure S7). Again, the agreement between measured and calculated m/z data is excellent, as attested by diamine-capped $[PPG_{30} + Na + NH_4]^{2+}$ which is observed at m/z 943.182 and has a theoretical m/z value of 943.188.

A third PPG distribution is observed in LC-IM band 2, located in the 2D LC-IM mobilogram between bands 1 and 3 (cf. Figure 5c). The m/z data of its n-mers in the extracted mass spectrum (Figure 6b) agree well with sodiated PPG chains H/OH end groups (total end group mass of 18 Da). The measured and calculated m/z values of the 16-mer from this distribution are 969.671 and 969.670, respectively (within 1 ppm), corroborating the assigned composition.

LC-IM bands 4a and 4b exhibit very similar LC-IM (i.e., polarity and ion mobility) characteristics but are still sufficiently separated to allow for extraction of individual mass spectra, which are shown in Figure 7a,b. Both these spectra contain oligomer distributions with a repeat unit mass of 28 Da, which is diagnostic of PE. As mentioned before, PE is difficult to ionize by ESI, unless it is functionalized with heteroatoms that can bind a proton or metal ion. The m/z data of the peaks present in Figure 7a are consistent with [M + Na] ions of oxidized PE chains with the composition H- $[CH_2CH_2]_n$ – $[CH_2CH(OH)]_4$ – H and a summed end group and substituent mass of 66 Da; similarly, the m/z data in Figure 7b agree well with the composition $H-[CH_2CH_2]_n$ [CH₂CH(OH)]₃-H and a summed end group and substituent mass of 50 Da (see also Figure S8). Such PE chains can arise by oxidation of their CH₂ to CH(OH) groups. ESI is a soft ionization method that generally does not alter analytes; hence, the oxidized PE species detected must have been formed in the vehicular engine, 44,45 from PE leaked into the additives (vide supra). It is noteworthy that the PE chains detected by ASAP-MS are more highly oxidized (cf. Figure S3), documenting that further oxidation can occur upon ASAP-MS. 46 The oxidized CH(OH) units are probably distributed randomly along the PE chain.

The polymeric components of the engine deposit identified by LC-IM-MS are amphiphilic oligomers. Their poor fractionation upon RP-LC (cf. Figure 5a) is consistent with comparable polarities; hence, the separation achieved after 2D LC-MS must be due to unique ion mobilities of the ions formed from the coeluting mixtures. In IM experiments, ions travel through an electric field, applied to a cell filled with a bath gas. 50 The field propels the ions forward, while ion collisions with the bath gas slow down this forward motion. The drift time through the IM cell depends on the ions' charge and size/shape as described by their collision cross-section (CCS). Generally, ions in higher charge states and with smaller CCS drift faster than ions with the opposite features. 32,35,48-50 Table 3 summarizes the measured drift times of ions formed from the oligomers coeluting at 9.5-10.0 min (Figure 5a). Expectedly, doubly charged PPG diamine has a shorter drift time than all other ions which are singly charged. On the other hand, singly charged PPG diamine drifts faster than PPG with H/OH end groups in spite of its larger mass, most likely because intramolecular interactions between its amine end groups give rise to a more compact conformation than that of PPG with H/OH end groups. Finally, the two oxidized PE chains, should have rather linear conformations, similar to that of PPG with water end groups; their lower drift times reflect the much smaller mass of the PE chains eluting at the same time as PPG with H/OH end groups. Very similar trends are observed for the mixtures coeluting at other retention times.

The foregoing discussion highlights the benefit of using two orthogonal separation techniques, viz. ion mobility and liquid chromatography, when analyzing a complex mixture. LC gives rise to a broad peak for the polymeric constituents of the

Table 3. IM Drift Times of Ions from Oligomers Eluting in the LC Fraction at 9.5–10.0 min

IM-MS band	oligomer ion ^{a,b}	m/z	mass (Da)	drift time (ms)
1	H ₂ NCH ₂ CH ₂ - [OCH ₂ CH(CH ₃)] ₂₂ - OCH ₂ CH ₂ NH ₂ ^a	1404.0	1404.0	8.7
2	$H-[OCH_2CH(CH_3)]_{16}-OH^a$	969.7	969.7	13.6
3	H ₂ NCH ₂ CH ₂ - [OCH ₂ CH(CH ₂)] ₂₃ - OCH ₂ CH ₂ NH ₂ ^B	742.5	1485.0	8.2
4a	$H-[CH_2CH_2]_{17}-[CH_2CH(OH)]_4-H^a$	677.6	677.6	9.5
4b	$H-[CH_2CH_2]_{19}-[CH_2CH(OH)]_3-H^a$	689.6	689.6	9.7
a[M + N]	$[Ma]^{+}$ ions. $[M + 2Na]^{2+}$ ions.			

engine deposit (Figure 5a). Without further separation, differentiation of the polymer distributions present is difficult, as multiple homopolymers and their respective charge states are superimposed (Figure 5b). 2D LC-IM dispersion combined with ESI-MS helped to resolve this problem, enabling the identification of several low molecular weight polymers. Among them, a new PPG with water (H/OH) end groups was observed, which is different than the PPG detected via MALDI-MS. Further, the presence of oxidized polyethylene in the solid engine deposit, which was suggested by ASAP-MS, could be confirmed by LC-IM-MS.

CONCLUSIONS

In this study, deposits accumulated in the air in-take valve of vehicular engines were analyzed by a palette of mass spectrometry techniques, encompassing MALDI-MS with postacquisition Kendrick analysis, ASAP-MS, and LC-IM-MS. Collaboratively, these methods established that various low molecular weight polymers often added to (or leaked into) fuel or lubricants are also present in the deposits, including PPG, PMMA, PIB, and PE.

The composition of polymer blends that give convoluted mass spectra could be effectively visualized by postacquisition Kendrick analysis using fractional base units. Our study also affirmed that different mass spectrometry techniques can be used cooperatively, either in series (as in LC-IM-MS) or in parallel (as in MALDI-MS vs ASAP-MS vs LC-MS), for the elucidation of complex fuels and fuel byproducts; this approach, which had been applied previously to fuels and fuel additives, ^{17,19,20,22,26} was successfully extended in this study for the first time to vehicular engine deposits. Overall, specific low molecular weight polymer structures could be detected and identified in a completely unknown sample that was examined using various separation methods and accurate mass measurements. Such information is more challenging to acquire, but definitely more insightful as compared to analyses that only report molecular weight distributions or analyses of known and purposely prepared mixtures. The drawback of investigating a complete unknown is that it is difficult to ensure that all ingredients are elucidated.

The (macro)molecular components found in the deposit are polar or amphiphilic; thus, they contain the structural features needed to develop noncovalent intermolecular interactions, via hydrogen bonding, electrostatic attraction, and/or coacervation, which are thought to be the cause of deposition/particulate accumulation in vehicular engines.¹⁷ Assessing the

nature of the polar or amphiphilic components present in these deposits provides a better understanding of these unintended byproduct buildups and facilitates progress toward their prevention.

ASSOCIATED CONTENT

5 Supporting Information

The Supporting Information is available free of charge at https://pubs.acs.org/doi/10.1021/acs.energyfuels.0c02702.

Kendrick plot with R = 58.04186 (Figure S1); ASAP-MS spectra of engine deposit after isothermic heating for 2–6 and 6–10 min (Figure S2); ASAP-MS spectra of engine deposit after isothermic heating for 10–14 min (Figure S3); LC-MS spectrum of the fraction eluting at 1.68 min (Figure S4); LC-MS spectrum of the fraction eluting at 4.25 min (Figure S5); 2D LC-IM mobilogram of the engine deposit using warmer colors (Figure S6); isotope clusters in the LC-IM-MS spectra of bands 1 and 3 (Figure S7); isotope clusters in the LC-IM-MS spectra of bands 4a and 4b (Figure S8) (PDF)

AUTHOR INFORMATION

Corresponding Author

Chrys Wesdemiotis — Department of Chemistry, Knight Chemical Laboratory, The University of Akron, Akron, Ohio 44325, United States; orcid.org/0000-0002-7916-4782; Email: wesdemiotis@uakron.edu

Author

Savannah R. Snyder – Department of Chemistry, Knight Chemical Laboratory, The University of Akron, Akron, Ohio 44325, United States

Complete contact information is available at: https://pubs.acs.org/10.1021/acs.energyfuels.0c02702

Notes

The authors declare no competing financial interest.

ACKNOWLEDGMENTS

This project was supported by the National Science Foundation (Grant No. CHE-1808115).

REFERENCES

- (1) Sperling, D.; Gordon, D. Two Billion Cars: Driving Toward Sustainability; Oxford University Press: New York, 2010.
- (2) Jatana, G. S.; Splitter, D. A.; Kaul, B.; Szybist, J. P. Fuel property effects on low-speed pre-ignition. *Fuel* **2018**, *230*, 474–482.
- (3) Zahdeh, A.; Rothenberger, P.; Nguyen, W.; Anbarasu, M.; Schmuck-Soldan, S.; Schaefer, J.; Goebel, T. Fundamental approach to investigate pre-ignition in boosted SI engines. *SAE Int. J. Engines* **2011**, *4* (1), 246–273.
- (4) Dingle, S. F.; Cairns, A.; Zhao, H.; Williams, J.; Williams, O.; Ali, R. Lubricant induced pre-ignition in an optical SI engine. SAE Tech. Pap. Ser. 2014, 1222.
- (5) Zaccardi, J.-M.; Escudié, D. Overview of the main mechanisms triggering low-speed pre-ignition in spark-ignition engines. *Int. J. Engine Res.* **2015**, *16* (2), 152–165.
- (6) Georgi, C. W. Motor Oils and Engine Lubrication; Reinhold: New York, 1950.
- (7) Haenel, P.; Seyfried, P.; Kleeberg, H.; Tomazic, D. Systematic approach to analyze and characterize pre-ignition events in turbocharged direct-injected gasoline engines. SAE Tech. Pap. Ser. 2011, 0343.

- (8) Okada, Y.; Miyashita, S.; Izumi, Y.; Hayakawa, Y. Study of low-speed pre-ignition in boosted spark ignition engine. *SAE Int. J. Engines* **2014**, 7 (2), 584–594.
- (9) Wang, Z.; Qi, Y.; Liu, H.; Long, Y.; Wang, J.-X. Experimental study of pre-ignition and super-knock in gasoline engine combustion with carbon particle at elevated temperatures and pressures. *SAE Tech. Pap. Ser.* **2015**, 0752.
- (10) Gupta, A.; Seeley, R.; Shao, H.; Remias, J. Impact of particle characteristics and engine conditions on deposit-induced pre-ignition and superknock in turbocharged gasoline engines. *SAE Int. J. Fuels Lubr.* 2017, 10 (3). DOI: 10.4271/2017-01-2345.
- (11) Parsinejad, F.; Biggs, W. Direct injection spark ignition engine deposit analysis: Combustion chamber and intake valve deposits. *SAE Tech. Pap. Ser.* **2011**, 2110.
- (12) Edney, M. K.; Barker, J.; Reid, J.; Scurr, D. J.; Snape, C. E. Recent advances in the analysis of GDI and diesel fuel injector deposits. *Fuel* **2020**, 272, 117682.
- (13) King, R. Understanding engine oils. https://www.penriteoil.com.au/assets/pdf/tech/Nov2015/Engine_Oils.pdf (accessed on 21 June 2020).
- (14) Zoller, U., Ed.; Handbook of Detergents Part E: Applications; CRC: Boca Raton, FL, 2009; Vol. 141.
- (15) Michael, P. W.; Wanke, T. S.; McCambridge, M. A.; Tung, S.; Kinker, B.; Woydt, M.; Dean, S. W. Additive and base oil effects in automatic particle counters. *J. ASTM Int.* **2007**, *4* (4), 100941.
- (16) Ruppel, T. D.; Hall, G. Determination of ethylene glycol in used engine oil by headspace-gas chromatography. *Perkin Elmer Application Note*, 2005; https://www.perkinelmer.com/lab-sol.utions/resources/docs/APP_Determination-of-Ethylene-Glycol-012090_01.pdf (accessed on 21 June 2020).
- (17) Johnson, D. W. Applications of mass spectrometric techniques to the analysis of fuels and lubricants. Mass Spectrometry (Chapter 7). In *Mass Spectrometry*; Aliofkhazraei, M., Ed.; InTechOpen, 2017; pp 209–228.
- (18) Huang, J. K. C.; Chen, R.; Loran, C. Analysis of high boiling components in petroleum products by LC/MS. *Thermo Scientific Application Note* 341, 2007; https://assets.thermofisher.com/TFS-Assets/CMD/Application-Notes/an-371-lc-ms-high-boiling-components-petroleum-an62497-en.pdf (accessed on 21 June 2020).
- (19) Bae, E. J.; Na, J.-G.; Chung, S. H.; Kim, H. S.; Kim, S. Identification of about 30 000 chemical components in shale oils by electrospray ionization (ESI) and atmospheric pressure photoionization (APPI) coupled with 15 T Fourier transform ion cyclotron resonance mass spectrometry (FT-ICR MS) and a comparison to conventional oil. *Energy Fuels* **2010**, *24* (4), 2563–2569.
- (20) Wang, S.-Z.; Fan, X.; Zheng, A.-L.; Wang, Y.-G.; Dou, Y.-Q.; Wei, X.-Y.; Zhao, Y.-P.; Wang, R.-Y.; Zong, Z.-M.; Zhao, W. Evaluation of atmospheric solids analysis probe mass spectrometry for the analysis of coal-related model compounds. *Fuel* **2014**, *117* (A), 556–563.
- (21) Tose, L. V.; Murgu, M.; Vaz, B. G.; Romão, W. Application of atmospheric solids analysis probe mass spectrometry (ASAP-MS) in petroleomics: analysis of condensed aromatics standards, crude oil, and paraffinic fraction. *J. Am. Soc. Mass Spectrom.* **2017**, 28 (11), 2401–2407.
- (22) Zhu, J.-L.; Fan, X.; Wei, X.-Y.; Wang, S.-Z.; Zhu, T.-G.; Zhou, C.-C.; Zhao, Y.-P.; Wang, R.-Y.; Lu, Y.; Chen, L.; You, C.-Y. Molecular characterization of heteroatomic compounds in a high-temperature coal tar using three mass spectrometers. *Fuel Process. Technol.* **2015**, *138*, 65–73.
- (23) McEwen, C. N.; McKay, R. G.; Larsen, B. S. Analysis of solids, liquids, and biological tissues using solids probe introduction at atmospheric pressure on commercial LC/MS instruments. *Anal. Chem.* **2005**, 77 (23), 7826–7831.
- (24) Smith, M. J. P.; Cameron, N. R.; Mosely, J. A. Evaluation atmospheric pressure solids analysis probe (ASAP) mass spectrometry for the analysis of low molecular weight synthetic polymers. *Analyst* **2012**, *137* (19), 4524–4530.

- (25) Barrère, C.; Hubert-Roux, M.; Afonso, C.; Racaud, A. Rapid analysis of lubricants by atmospheric solid analysis probe-ion mobility mass spectrometry. *J. Mass Spectrom.* **2014**, 49 (8), 709–715.
- (26) Beaumesnil, M.; Mendes Siqueira, A. L.; Hubert-Roux, M.; Loutelier-Bourhis, C.; Afonso, C.; Racaud, A.; Bai, Y. Highperformance thin-layer chromatography with atmospheric solids analysis probe mass spectrometry for analysis of gasoline polymeric additives. *Rapid Commun. Mass Spectrom.* 2020, Ahead of Print. DOI: 10.1002/rcm.8755.
- (27) Amundson, L. M.; Gallardo, V. A.; Vinueza, N. R.; Owen, B. C.; Reece, J. N.; Habicht, S. C.; Fu, M.; Shea, R. C.; Mossman, A. B.; Kenttämaa, H. I. Identification and counting of oxygen functionalities and alkyl groups of aromatic analytes in mixtures by positive-mode atmospheric pressure chemical ionization tandem mass spectrometry coupled with high-performance liquid chromatography. *Energy Fuels* **2012**, *26* (5), 2975–2989.
- (28) Dhungana, B.; Becker, C.; Zekavat, B.; Solouki, T.; Hockaday, W. C.; Chambliss, C. K. Characterization of slow-pyrolysis bio-oils by high-resolution mass spectrometry and ion mobility spectrometry. *Energy Fuels* **2015**, *29* (2), 744–753.
- (29) Fouquet, T.; Sato, H. Extension of the Kendrick mass defect analysis of homopolymers to low resolution and high mass range mass spectra using fractional base units. *Anal. Chem.* **2017**, 89 (5), 2682–2686.
- (30) Fouquet, T.; Nakamura, S.; Sato, H.; Cody, R. Real divisors and pseudocontinuous enhancement of resolution for a Kendrick mass defect analysis. *Rapid Commun. Mass Spectrom.* **2019**, 33 (19), 1547–1551.
- (31) Fouquet, T. The Kendrick analysis for polymer mass spectrometry. J. Mass Spectrom. 2019, 54, 933-947.
- (32) Pringle, S. D.; Giles, K.; Wildgoose, J. L.; Williams, J. P.; Slade, S. E.; Thalassinos, K.; Bateman, R. H.; Bowers, M. T.; Scrivens, J. An investigation of the mobility separation of some peptide and protein ions using a new hybrid quadrupole/travelling wave IMS/oa-ToF instrument. *Int. J. Mass Spectrom.* **2007**, *261*, 1–12.
- (33) Li, L., Ed.; MALDI Mass Spectrometry for Synthetic Polymer Analysis; John Wiley & Sons: Hoboken, NJ, 2011.
- (34) Barner-Kowollik, C.; Gruendling, T.; Falkenhagen, J.; Weidner, S., Eds.; *Mass Spectrometry in Polymer Chemistry*; Wiley-VCH Verlag: Weinheim, Germany, 2012.
- (35) Wesdemiotis, C. Multidimensional mass spectrometry of synthetic polymers and advanced materials. *Angew. Chem., Int. Ed.* **2017**, *56* (6), 1452–1464.
- (36) Wollyung, K. M.; Wesdemiotis, C.; Nagy, A.; Kennedy, J. P. Synthesis and mass spectrometry characterization of centrally and terminally amine-functionalized polyisobutylenes. *J. Polym. Sci., Part A: Polym. Chem.* **2005**, 43 (5), 946–958.
- (37) Huo, X.; Shi, Z.; Cheng, H. C.; Sun, X.; Ma, S. Fuel additive, and preparation method and usage method thereof. *PCT Int. Appl.* 2017, WO Patent 2017075197 A1 WO 20170504. https://patents.google.com/patent/WO2017075197A1/en (accessed on 4 July 2020).
- (38) Sato, H.; Nakamura, S.; Teramoto, K.; Sato, T. Structural characterization of polymers by MALDI spiral-TOF mass spectrometry combined with Kendrick mass defect analysis. *J. Am. Soc. Mass Spectrom.* **2014**, 25 (8), 1346–1355.
- (39) Fouquet, T.; Sato, H. Improving the resolution of Kendrick mass defect analysis for polymer ions with fractional base units. *Mass Spectrom.* **2017**, *6* (1), A0055.
- (40) Jarvik, O.; Oja, V. Molecular weight distributions and average molecular weights of pyrolysis oils from oil shales: literature data and measurements by size exclusion chromatography (SEC) and atmospheric solids analysis probe mass spectrometry (ASAP MS) for oils from four different deposits. *Energy Fuels* **2017**, 31 (1), 328–339.
- (41) Tose, L. V.; Murgu, M.; Vaz, B. G.; Romao, W. Application of atmospheric solids analysis probe mass spectrometry (ASAP-MS) in petroleomics: analysis of condensed aromatics standards, crude oil,

- and paraffinic fraction. J. Am. Soc. Mass Spectrom. 2017, 28 (11), 2401-2407.
- (42) Wolf, J.-C.; Gyr, L.; Mirabelli, M. F.; Schaer, M.; Siegenthaler, P.; Zenobi, R. A radical-mediated pathway for the formation of [M + H]⁺ in dielectric barrier discharge ionization. *J. Am. Soc. Mass Spectrom.* **2016**, 27 (9), 1468–1475.
- (43) Helps, I. G. Plastics in European Cars, 2000–2008: A Rapra Industry Analysis Report; RAPRA Technology: Shawbury, 2001.
- (44) Gatto, V.; Moehle, W.; Schneller, E.; Burris, T.; Cobb, T.; Featherstone, M.; Tung, S.; Kinker, B.; Woydt, M.; Dean, S. W. A review of engine oil oxidation bench tests and their application in the screening of new antioxidant systems for low phosphorus engine oils. *J. ASTM Int.* **2007**, *4* (7), 100849.
- (45) Mujahid, A.; Dickert, F. L. Monitoring automotive oil degradation: analytical tools and onboard sensing technologies. *Anal. Bioanal. Chem.* **2012**, 404 (4), 1197–1209.
- (46) Farenc, M.; Witt, M.; Craven, K.; Barrere-Mangote, C.; Afonso, C.; Giusti, P. Characterization of polyolefin pyrolysis species produced under ambient conditions by Fourier transform ion cyclotron resonance mass spectrometry and ion mobility-mass spectrometry. J. Am. Soc. Mass Spectrom. 2017, 28 (3), 507–514.
- (47) Uliyanchenko, E. Applications of hyphenated liquid chromatography techniques for polymer analysis. *Chromatographia* **2017**, *80*, 731–750.
- (48) Solak Erdem, N.; Alawani, N.; Wesdemiotis, C. Characterization of polysorbate 85, a nonionic surfactant, by liquid chromatography vs. ion mobility separation coupled with tandem mass spectrometry. *Anal. Chim. Acta* **2014**, 808, 83–93.
- (49) Crotty, S.; Gerislioglu, S.; Endres, K.; Wesdemiotis, C.; Schubert, U. S. Polymer architectures *via* mass spectrometry and hyphenated techniques. *Anal. Chim. Acta* **2016**, 932, 1–21.
- (50) Morris, C. B.; Poland, J. C.; May, J. C.; McLean, J. A. Fundamentals of ion mobility-mass spectrometry for the analysis of biomolecules. *Methods Mol. Biol.* **2020**, 2084, 1–31.